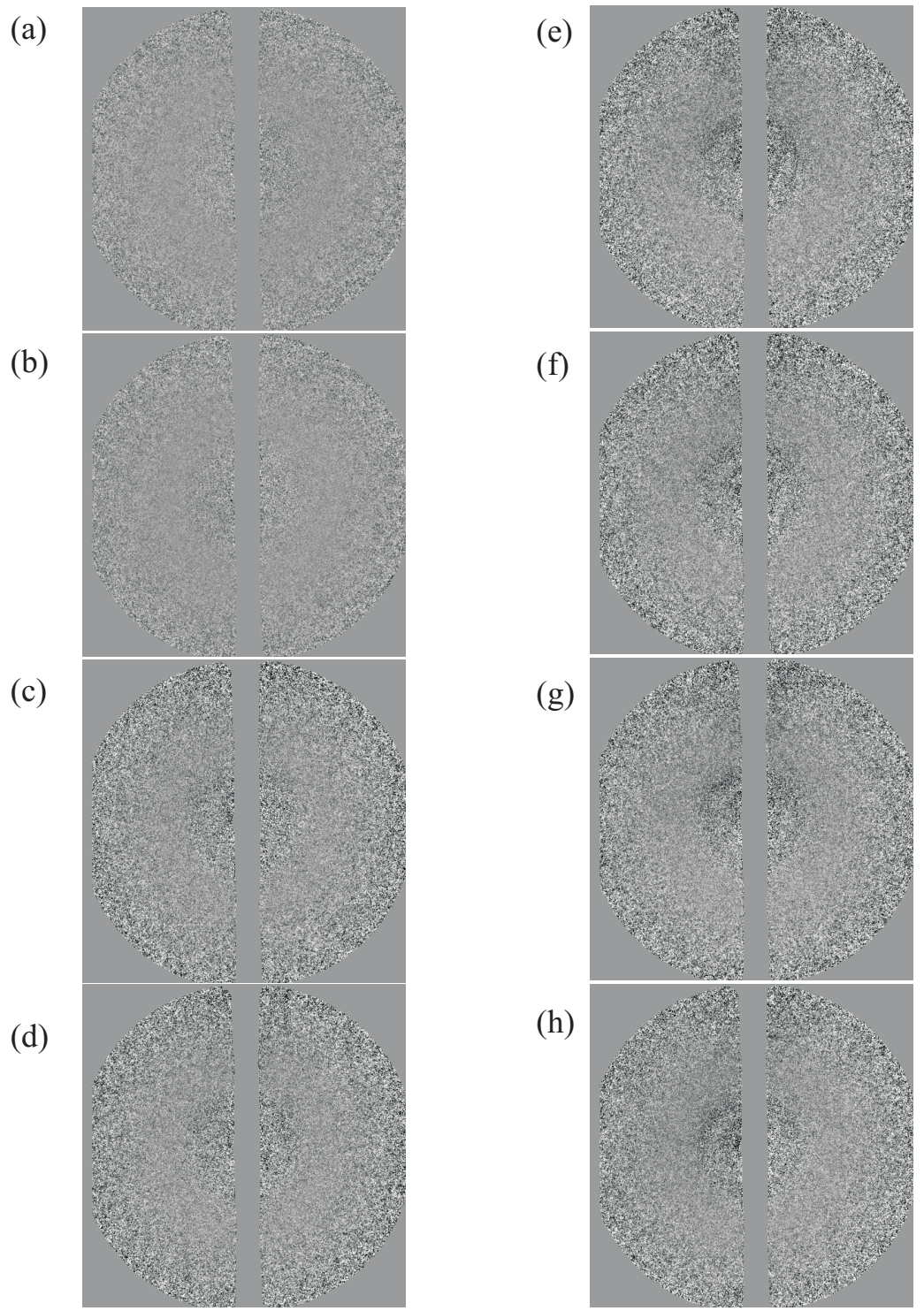

Fig.6-1. Difference patterns created by subtracting the ratio pattern of the –77 ps time point from the ratio patterns recorded at (a) –27 ps, (b) +13 ps, (c) +18 ps, (d) +23 ps, (e) +28 ps, (f) +33 ps, (g) +43 ps, and (h) +73 ps.

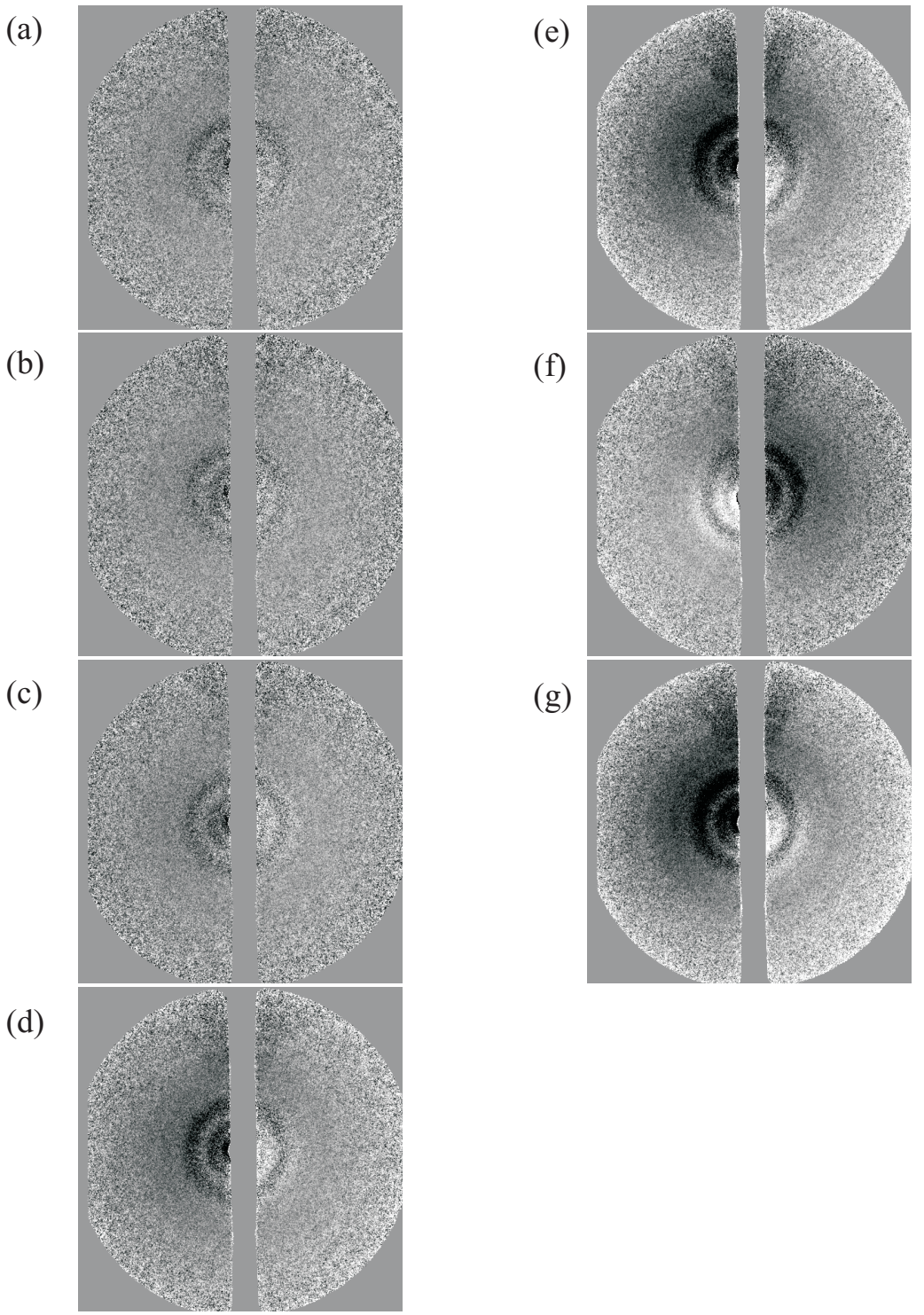

Fig.6-2. Difference patterns created by subtracting the ratio pattern of the –77 ps time point from the ratio patterns recorded at (a) +98 ps, (b) +123 ps, (c) +173 ps, (d) +223 ps, (e) +423 ps, (f) +823 ps, and (g) +1273 ps.

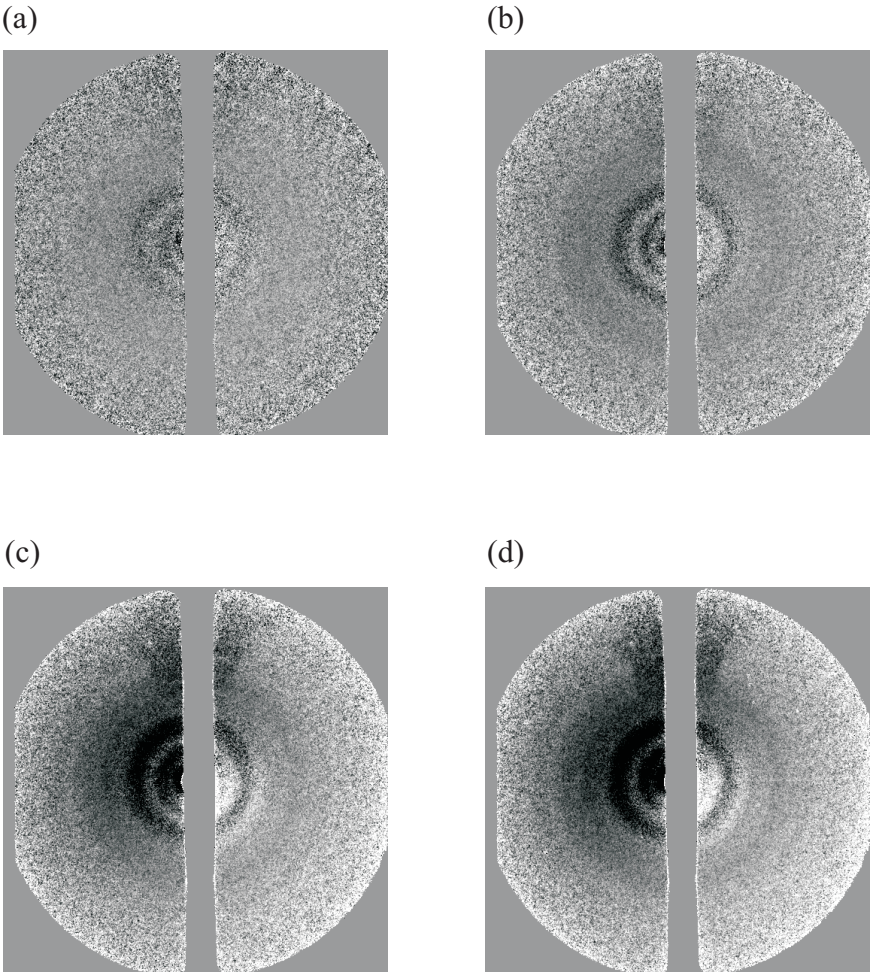

Fig.6-3. Comparison between data recorded with and without a neutral-density filter (10% transmission) in the beam path. Difference patterns are created by subtracting the ratio pattern of the –77 ps time point from the ratio patterns recorded at (a) +98 ps with laser filter, (b) +98 ps without laser filter, (c) +1273 ps with laser filter, and (d) +1273 ps without laser filter. The filtered data were used in the analysis reported herein.

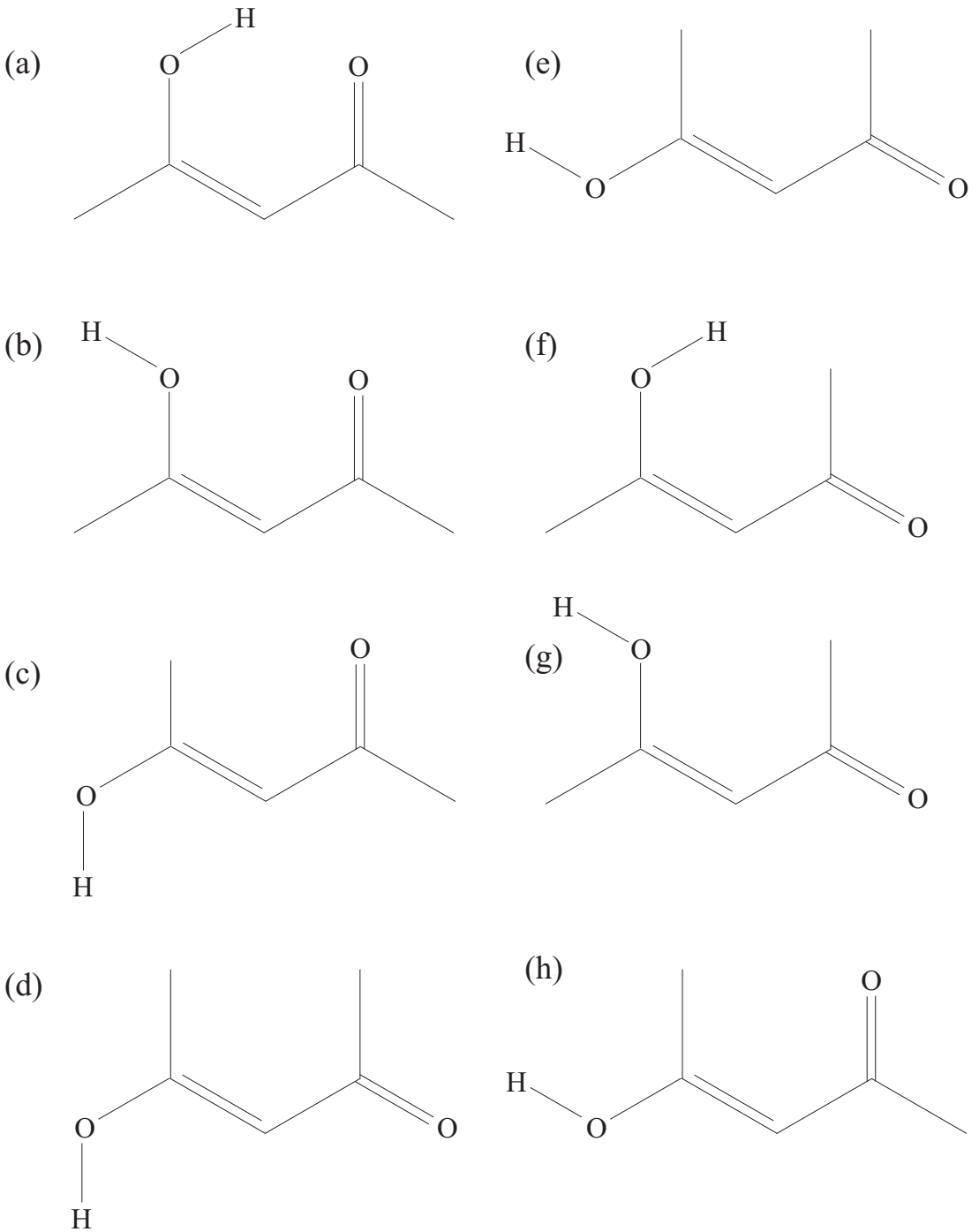

Fig.6-4. Isomers of the enol tautomer of acetylacetone. The naming convention is defined with respect to rotations about the C–O single bond, the C–C double bond, and the C–C single bond. C = cis; T = trans. (a) CCC, (b) TCC, (c) CTC (d) CTT, (e) TTT, (f) CCT, (g) TCT, (h) TTC.

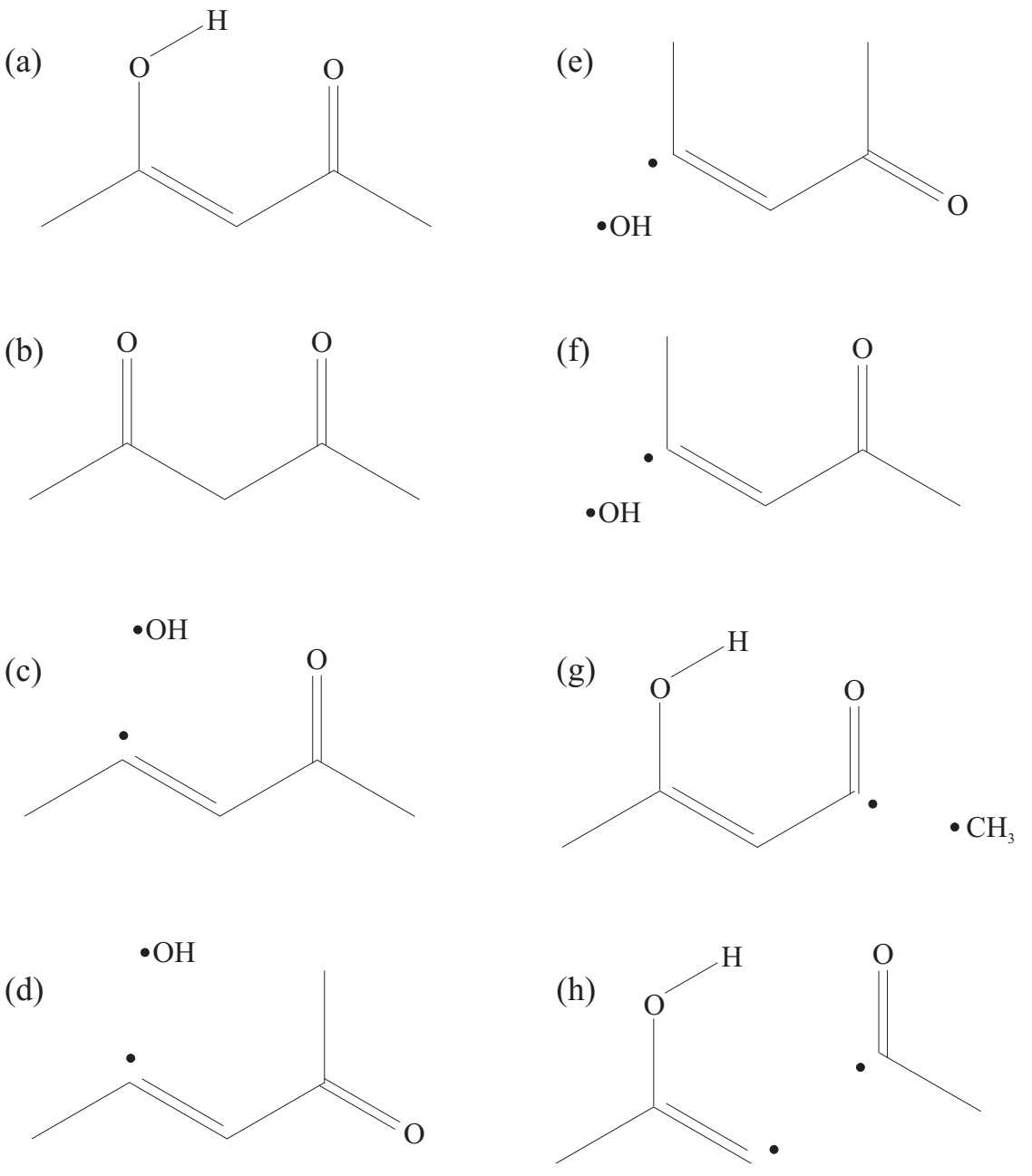

Fig. 6-5. Possible reaction products in the photolysis of (a) CCC enolic acetylacetone. (b) keto tautomer of acetylacetone. Four isomers of the 2-penten-4-on-2-yl radical + the OH radical (c) TC, (d) TT (e) CT, and (f) CC. (g) The CCC isomer of the formylacetonyl radical + the methyl radical. (h) The acetyl radical loss products.

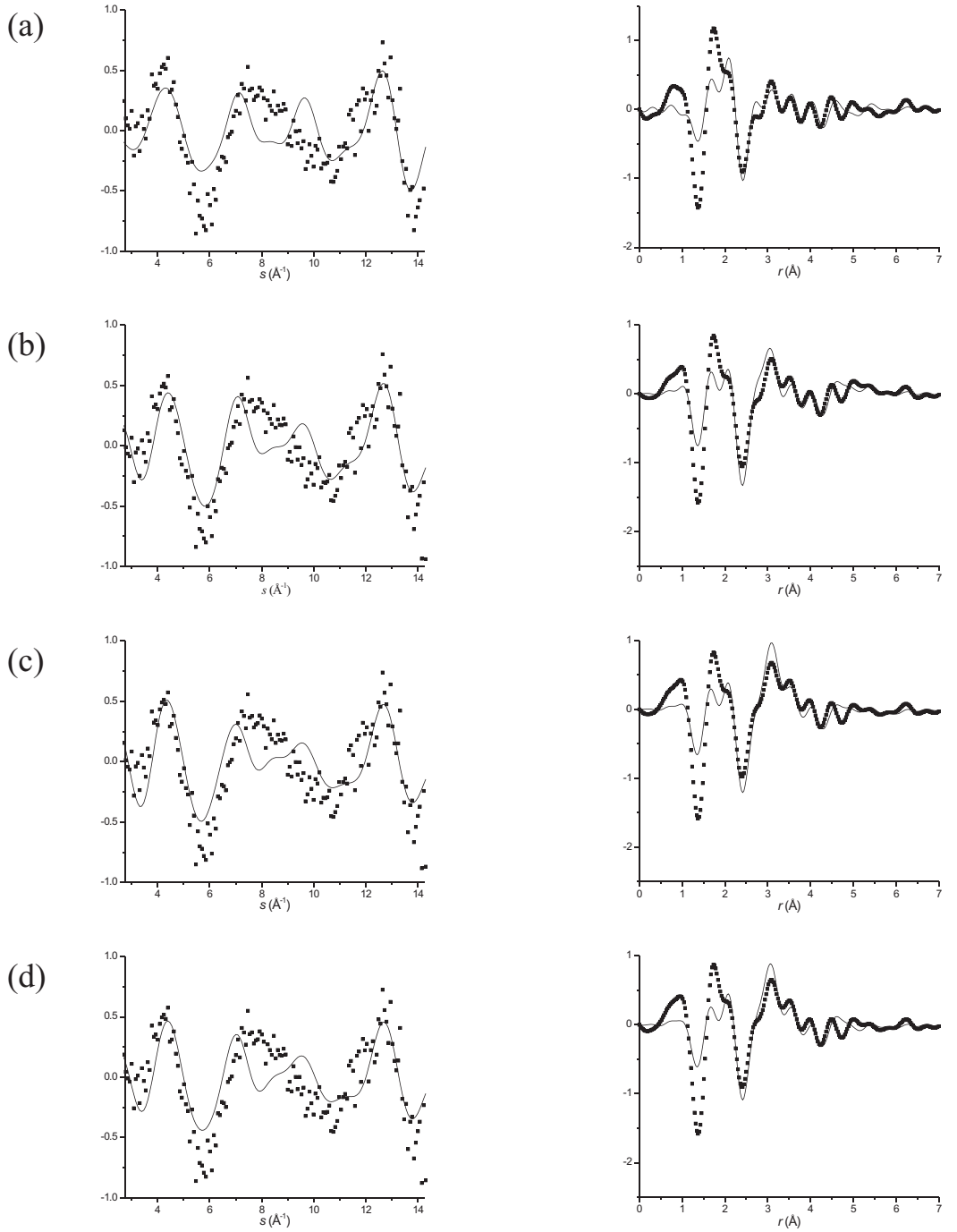

Fig. 6-6. Fits of possible reactions: left column $sM(s)$ and right column $f(r)$ having components' fractional contributions and polynomial background optimized. The data (squares) is the +1273 ps data point (t_{ref} = –77 ps) and theory (solid line) is derived from the DFT structures of possible products, here the enol isomers: (a) CCC, (b) TCC, (c) TCT, (d) TTC. ^{2} and R are given in Table 6-2.

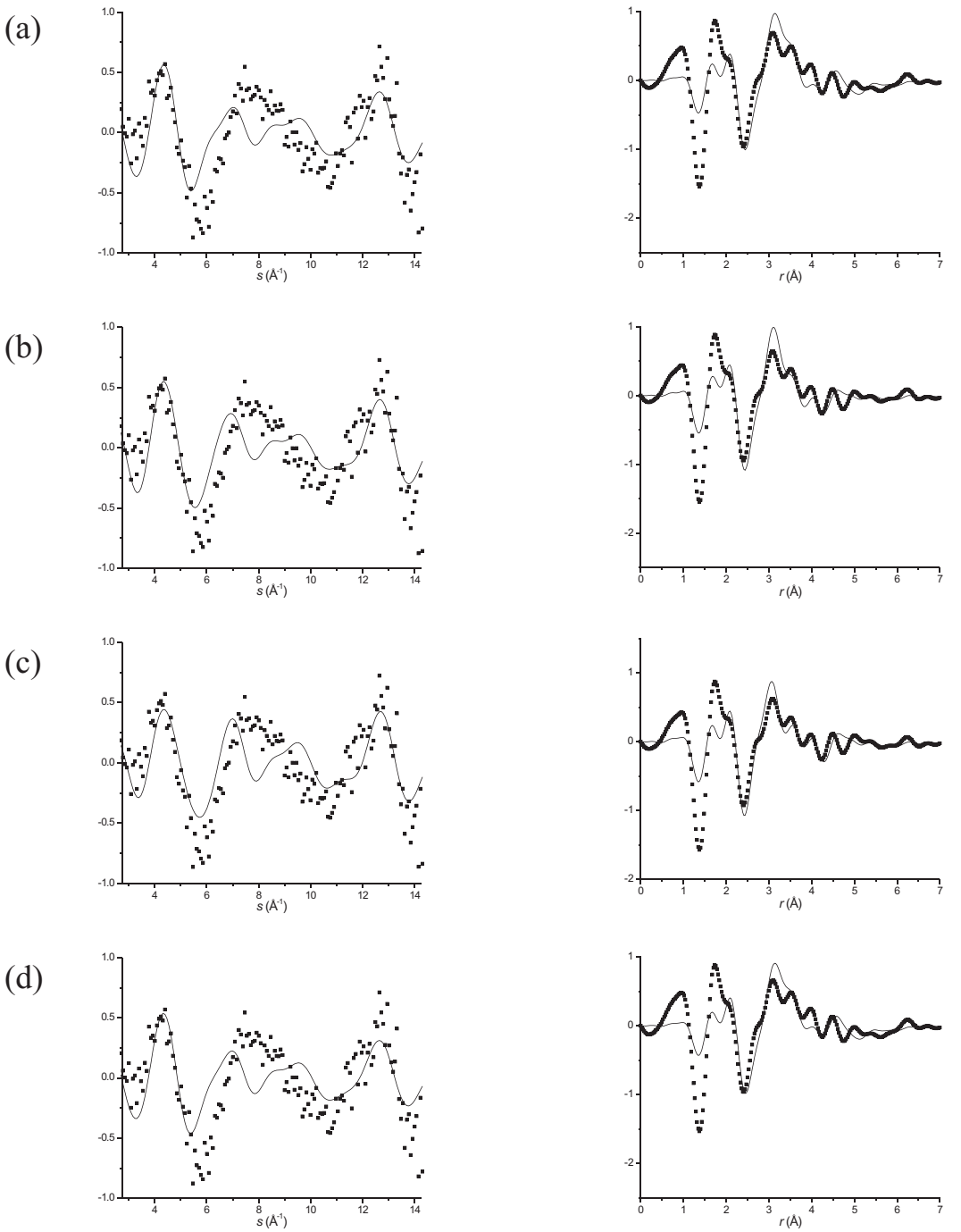

Fig. 6-7. Fits of possible reactions: left column $sM(s)$ and right column $f(r)$ having components' fractional contributions and polynomial background optimized. The data (squares) is the +1273 ps data point (t_{ref} = –77 ps) and theory (solid line) is derived from the DFT structures of possible products, here the enol isomers: (a) TTT, (b) CCT, (c) CTC, and (d) CTT. ^{2} and R are given in Table 6-2.

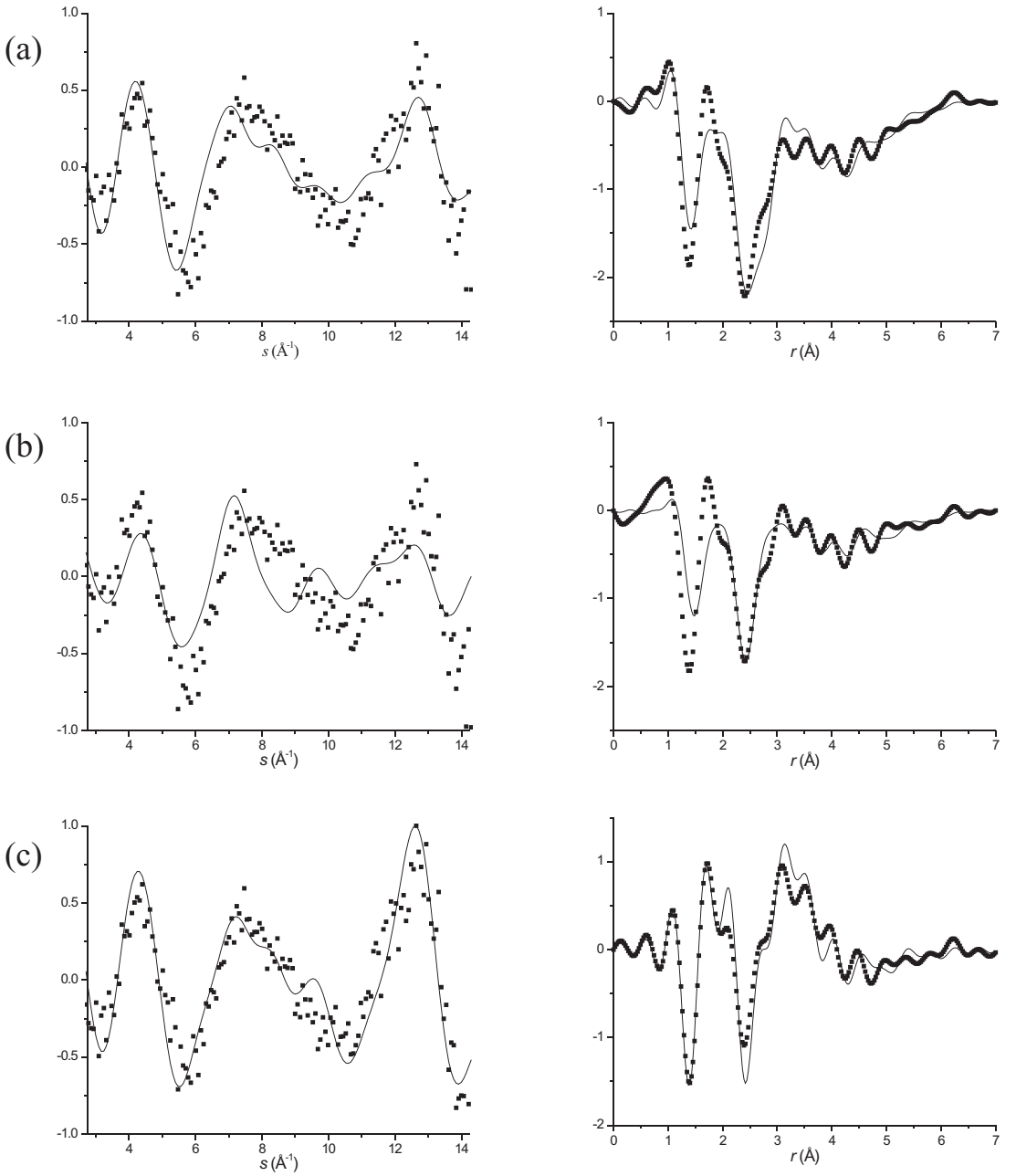

Fig. 6-8. Fits of possible reactions: left column $sM(s)$ and right column $f(r)$ having components' fractional contributions and polynomial background optimized. The data (squares) is the +1273 ps data point (t_{ref} = –77 ps) and theory (solid line) is derived from the DFT structures of possible products, here (a) a 1:1 mixture of vibrationally hot enol CCC and keto acetylacetone tautomers, (b) the methyl radical loss products, and (c) the acetyl radical loss products. ^{2} and R are given in Table 6-2.

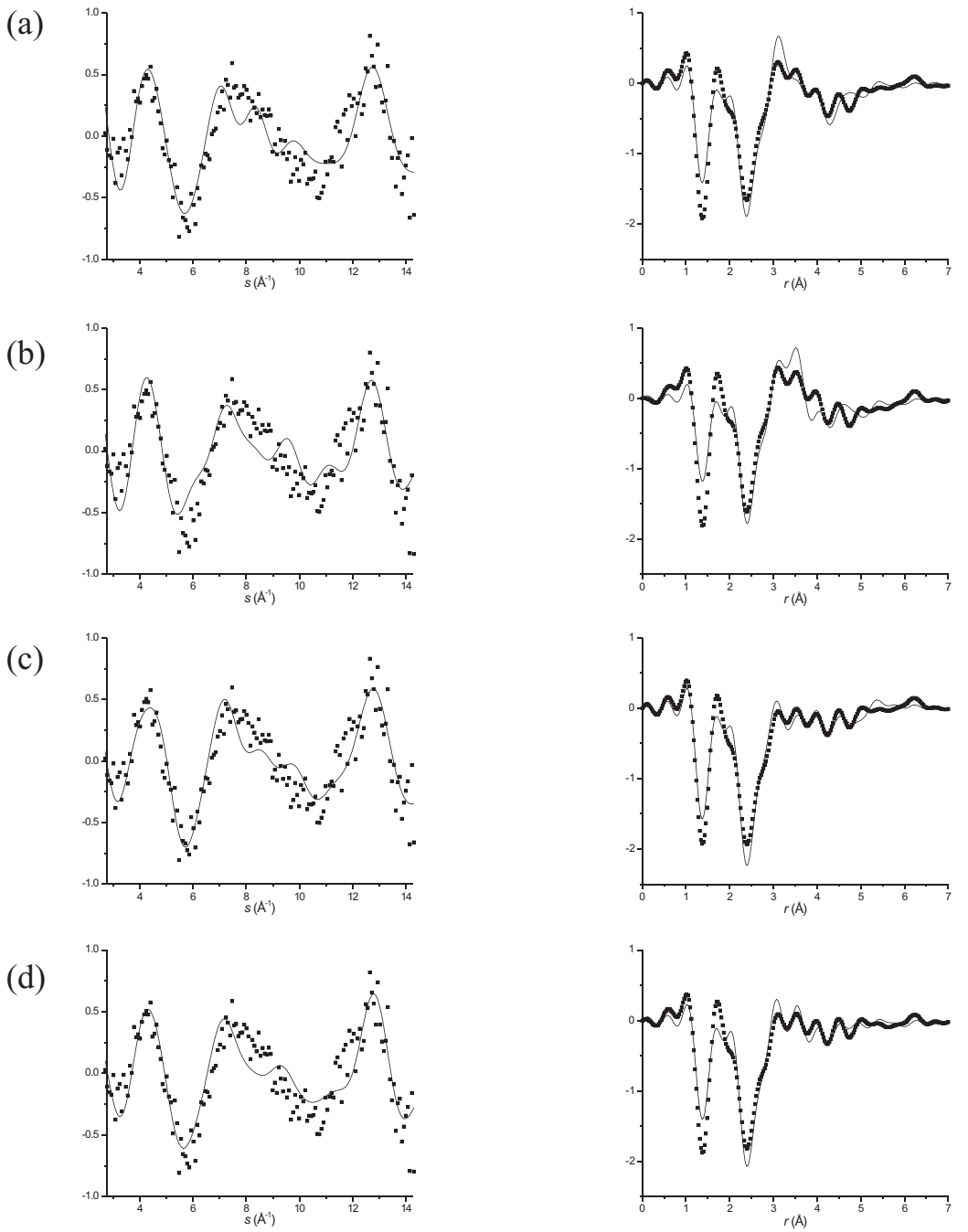

Fig. 6-9. Fits of possible reactions: left column $sM(s)$ and right column $f(r)$ having components' fractional contributions and polynomial background optimized. The data (squares) is the +1273 ps data point (t_{ref} = –77 ps) and theory (solid line) is derived from the DFT structures of possible products, here the OH loss products with the 2-penten-4-on-2-yl radical isomers (a) CC, (b) CT, (c) TC, (d) TT. ^{2} and R are given in Table 6-2.

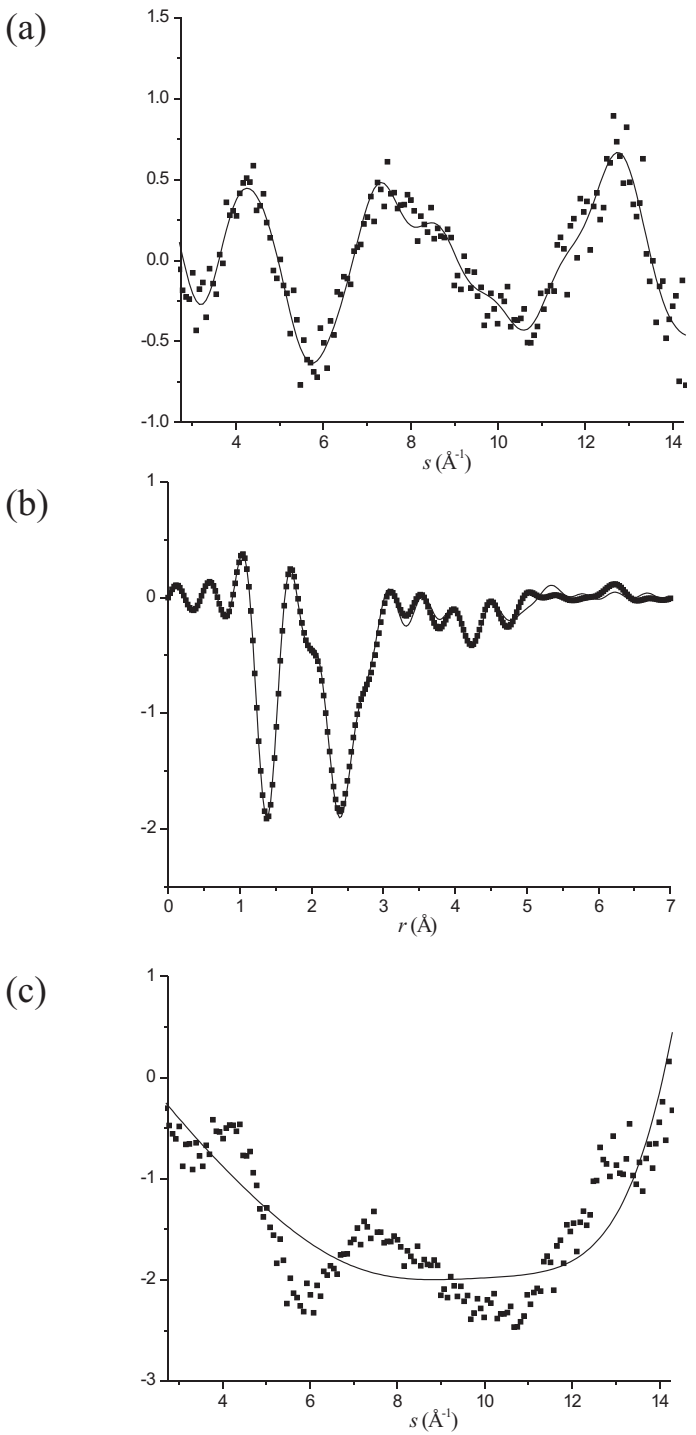

Fig. 6-10. The data (squares) and the refined theoretical model (line) corresponding to the reaction of enolic acetylacetone to form the TC 2-penten-4-on-2-yl and OH radicals. (a) $sM(s)$ comparison and (b) $f(r)$ comparison. (c) The experimental $sM(s)$ (squares) and the polynomial background (line). $^2 = 8.400$ and $R = 0.351$.

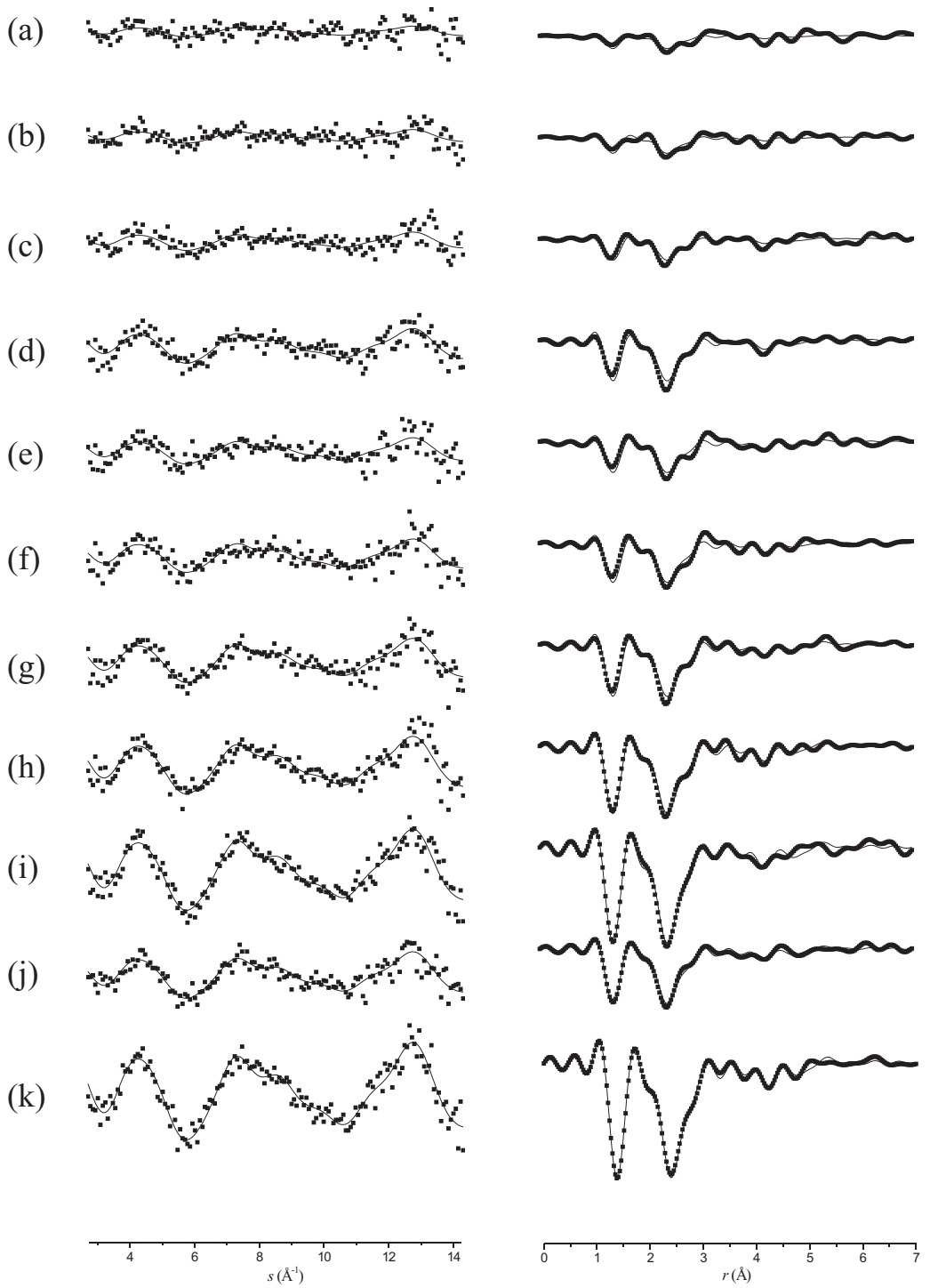

Fig. 6-11. The experimental (squares) and refined theoretical (solid line) $sM(s)$ (left) and $f(r)$ (right) at multiple time points (t_{ref} = –77 ps). t = (a) +28 ps, (b) +33 ps, (c) +43 ps, (d) +73 ps, (e) +98 ps, (f) +123 ps, (g) +173 ps, (h) +223 ps, (i) +423 ps, (j) +823 ps, (k) +1273 ps. Fitting information is given in Table 6-4.

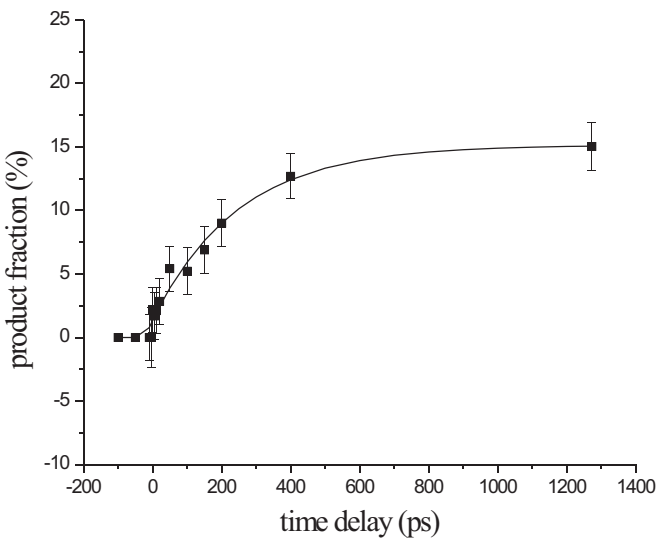

Fig. 6-12. The fit of a single-step reaction process (solid line) to the fraction of product structure at each time point (squares). The time constant for the reaction is 247 ± 34 ps.

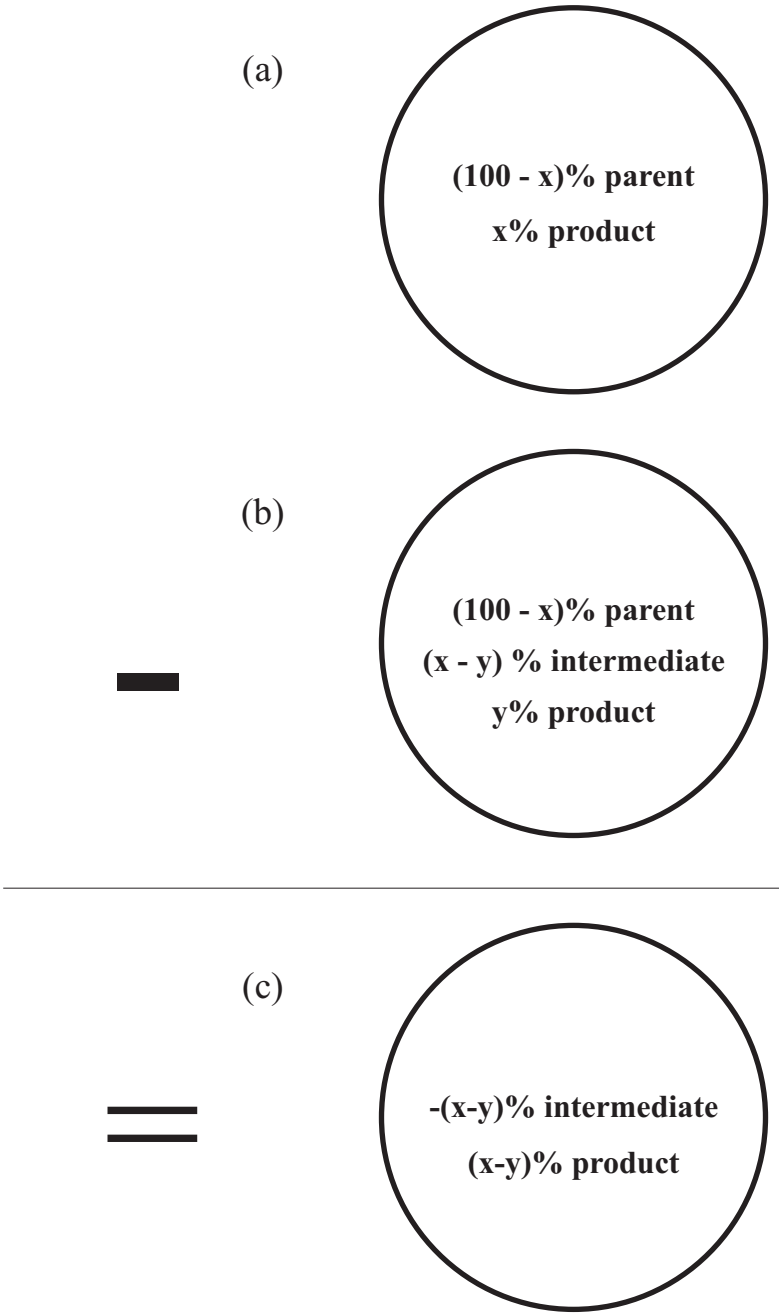

Fig. 6-13. A schematic illustration of the process used to isolate the reaction of the formation of product from an intermediate structure. Data from a time point (a) when the reaction is complete and only parent and product are present has data from an earlier positive time point (b) subtracted from it. This positive point contains unreacted parent, product, and reaction intermediate. The resulting difference data (c) has the parent contribution removed and contains only the structural information of product and intermediate molecules.

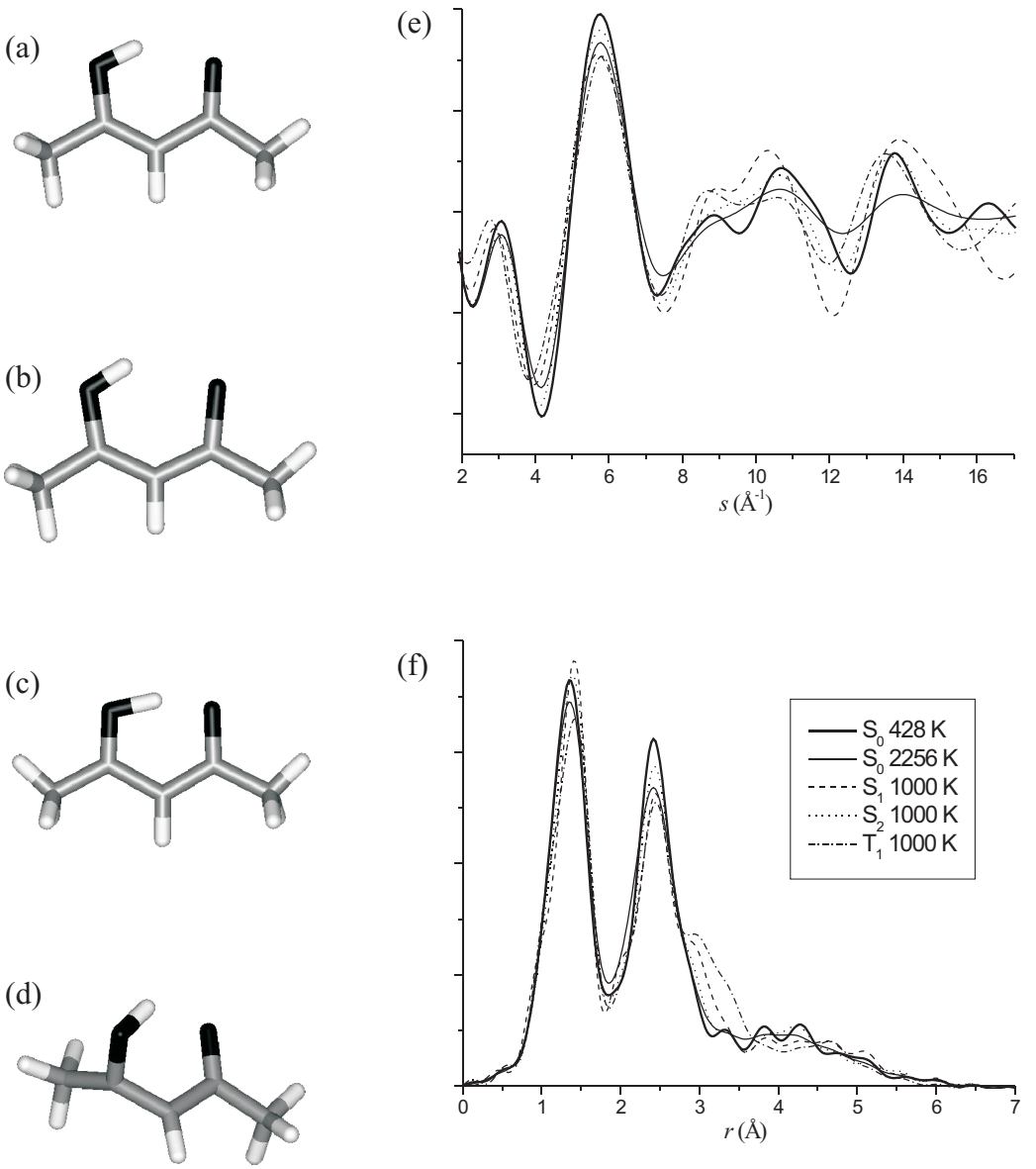

Fig. 6-14. The calculated molecular structure of some of the electronic states of enolic acetylacetone (a) S_0, (b) S_1 n *, (c) S_2 *, and (d) T_1 *. The (a) $sM(s)$ and (b) $f(r)$ curves calculated using these structures. S_0 at 428 K (broad solid line), S_0 at 2256 K (narrow solid line), S_1 at 1000 K (dashed line), S_2 at 1000 K (dotted line), and T_1 at 1000 K (dot-dash line).

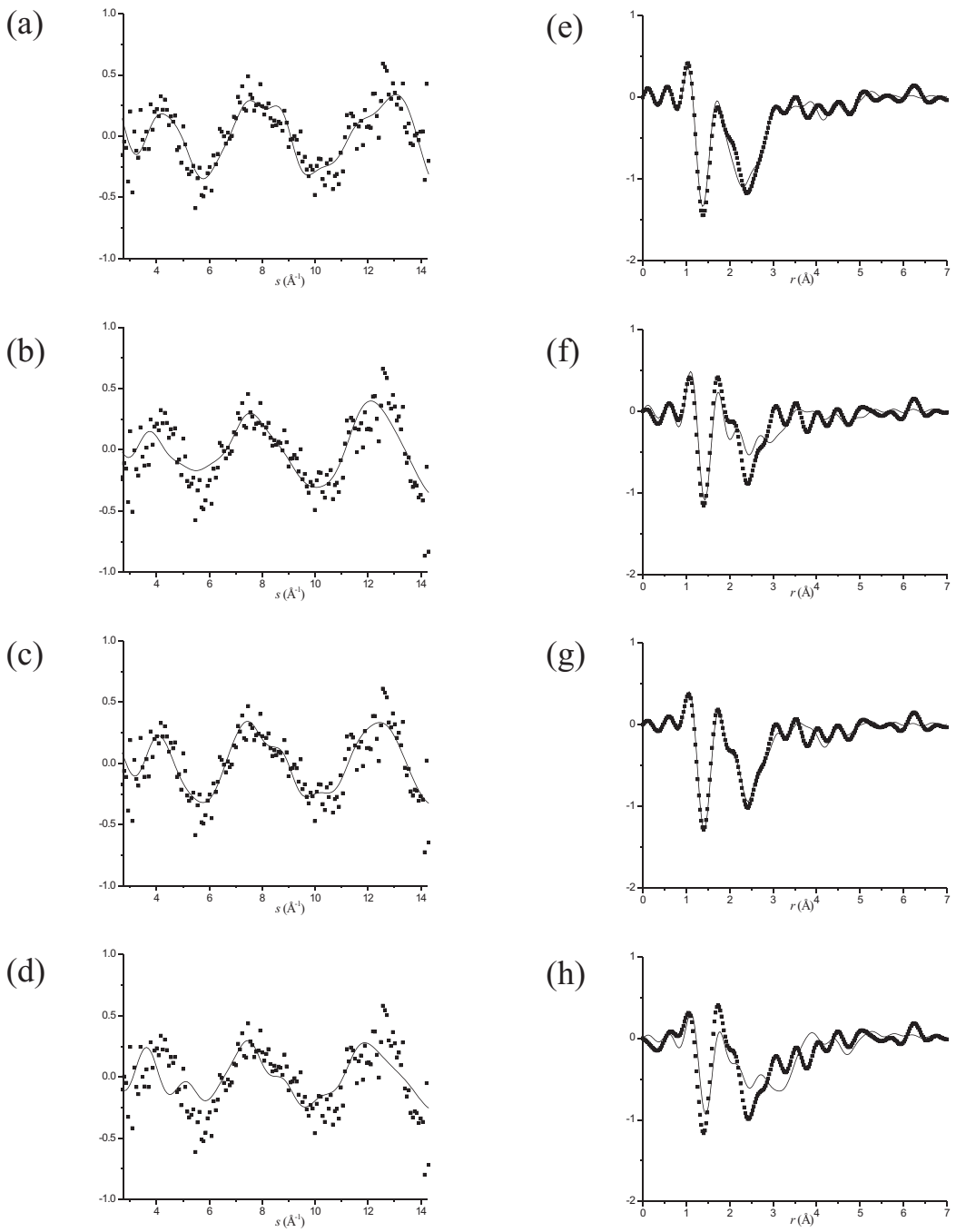

Fig. 6-15. The alternate $sM(s)$ (left) and $f(r)$ (right) created by subtracting the +73 ps time point from the +1273 ps time point. Here the experimental (squares) data is compared with theory (solid line) corresponding to the reaction of the intermediate to the refined product. The intermediate in each is represented by (a) enol S_0 at 2256 K, (b) enol S_1 at 1000 K, (c) enol S_2 at 1000 K, and (d) enol T_1 at 1000 K.

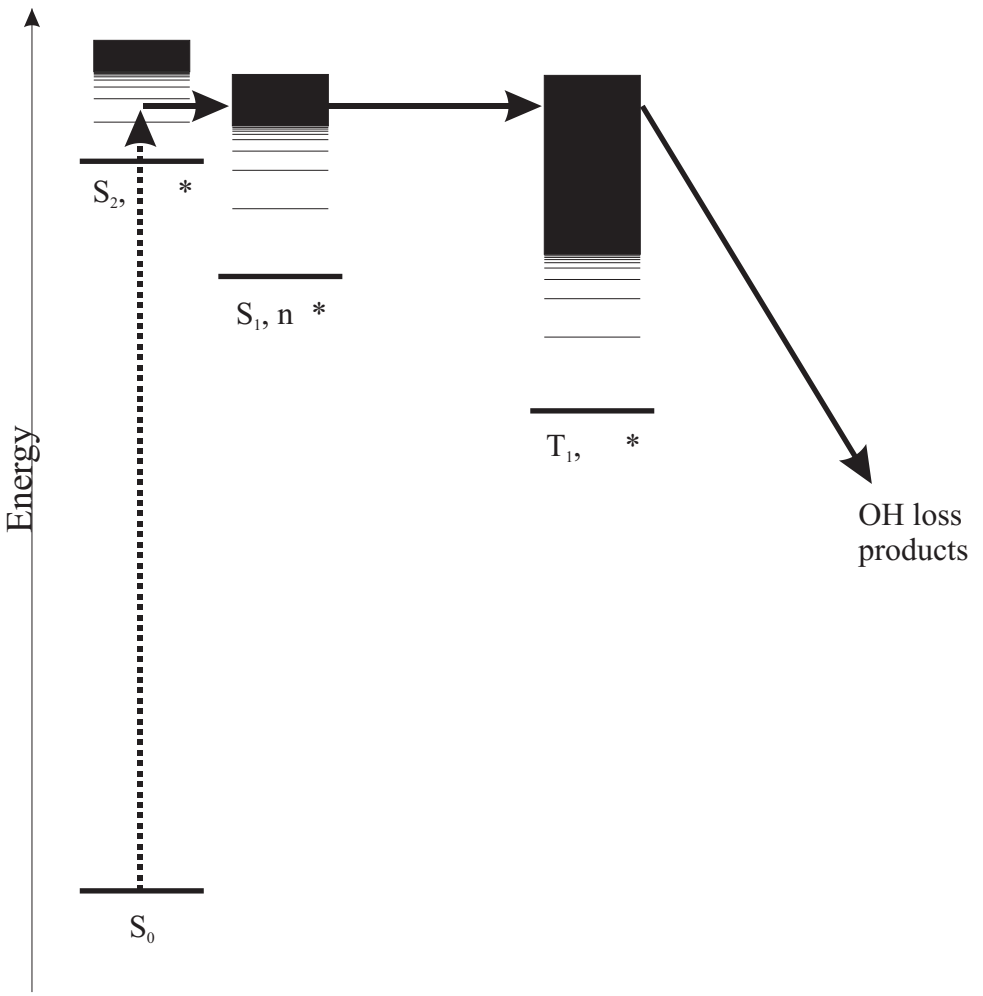

Fig. 6-16. The schematic representation of the dynamics of acetylacetone. Excited molecules arrive in the S_2 state where ultrafast internal conversion sends population to the S_1 state. Intersystem crossing to T_1 takes place over 247 ps ( ). Dissociation from T_1 to the radical products is then ultrafast such that its population never builds up enough to be detected by UED.